Retrieving PM10 Surface Concentration from AERONET Aerosol Optical Depth: The Cairo and Delhi Megacities Case Studies

Sara Said, Zeinab Salah, Mohamed Magdy Abdel Wahab, Stephane Alfaro

Journal of the Indian Society of Remote Sensing (August 2023) 51(8):1797–1807
https://doi.org/10.1007/s12524-023-01736-7

RESEARCH ARTICLE

Retrieving PM10 Surface Concentration from AERONET Aerosol Optical Depth: The Cairo and Delhi Megacities Case Studies

Sara Said[1] · Zeinab Salah[1] · Mohamed Magdy Abdel Wahab[2] · Stephane C. Alfaro[3]

Received: 31 October 2022 / Accepted: 6 July 2023 / Published online: 3 August 2023

Abstract

Large concentrations of air-suspended particulate matter (PM) in megacities represent an important health risk for their populations, but PM time series are often missing or too short to quantify the associated burden of diseases. In this study, we propose a model for retrieving the surface PM in Cairo (Egypt) and Delhi (India) from the automated measurements of aerosol optical depth (AOD), precipitable water (PW), and Angström exponent (AE) performed by the sunphotometers of the Aerosol Robotics Network (AERONET). For this we exploit the (1) synchronous measurements performed from 2010 to 2015 at the headquarters of the Egyptian Meteorological Authority and in 2009 at the Gual Pahari station (25 km south of Delhi) and (2) the ERA5 estimate of the planetary boundary layer height (H). The correlation between the surface PM10 and the AOD is primarily controlled by the variations of PW and secondarily by those of H: for similar surface PM10 concentrations, the AOD tends to be the largest in summer because of the hygroscopic enhancement of the mass extinction efficiency (σ) of the particles and their dilution in the more developed mixing layer. The variations of composition also play a significant role in Cairo. This effect, particularly marked in spring (coinciding with the dust season), can be parameterized as a linear function of AE. Finally, we show that the variations of the surface PM10 concentration at the two sites can be retrieved simply from those of the AOD, PW, AE and H. At the weekly temporal resolution, the agreement between the model and the observations is very good at the two locations (correlation coefficient > 0.81, relative mean absolute error $< 15\%$). This validates indirectly the assumption made in the development of the model, namely that the aerosols are mostly confined to the mixing layer of the two megacities and not transported in the free atmosphere. Provided a few years of surface PM measurements are available, the methodology proposed in this study could be easily applied to any other AERONET station.

Keywords Egypt · India · PM10 · Aerosol optical depth · Precipitable water · Angström exponent

Introduction

High levels of airborne particulate matter (PM or aerosols) have adverse effects on air quality and human health because they increase the risk of respiratory and cardiovascular diseases (Brauer et al., 2012; Brook et al., 2010; Kim et al., 2015; Prescott et al., 1998). Moreover, aerosols influence the Earth's climate directly by scattering and absorbing solar and terrestrial radiation (Sokolik & Toon, 1996) and indirectly by promoting or inhibiting the formation of clouds and changing their physical properties (Ramanathan et al., 2002).

Because the residence time of atmospheric particles in the troposphere is limited (from a few hours to a few days), their concentration and chemical or physical properties are highly variable in time and space. Therefore, documenting and understanding this variability requires to maintain perennial monitoring stations in a variety of regions with contrasted climatic and environmental conditions. In megacities, the concentrations are usually large and a network of monitoring stations would even be necessary to document their spatial variability (Wang & Christopher,

✉ Zeinab Salah
zeinabsalah@gmail.com

[1] Egyptian Meteorological Authority, Cairo, Egypt

[2] Cairo University, Giza, Egypt

[3] Université de Paris Est Créteil and Université de Paris Cité, CNRS, LISA, 94010 Créteil, France

2003). However, because of their cost such networks are either not deployed in the megacities of the developing countries or they do not have the required density. When they exist, the measurement datasets are also often too short to analyse the long-term evolution of the surface concentrations.

Hence, the importance of alternate methods is to estimate surface air quality in places where ground measurements are insufficient or lacking. Among these methods, the remote sensing of the atmosphere's composition is a promising tool. This explains that many studies have attempted to derive an estimate of the surface PM concentration from aerosol optical depth (AOD) measurements performed by satellite-borne instruments or, more rarely, ground-based sunphotometers (Barladeanu et al., 2012; Grguric et al., 2014; Guo et al., 2017; Handschuh et al., 2022; Kong et al., 2016; Lv et al., 2017; Ma, et al., 2016; Yahi et al., 2013; You et al., 2016; Zhang et al., 2021). An experimental linear model using only AOD as a PM predictor showed contrasted results. Indeed, the correlation coefficients between measured and predicted PM2.5 can vary between 0.2 and 0.75 (e.g. Chu et al., 2003; Engel-Cox et al., 2004; Gupta & Christopher, 2008; Wang & Christopher, 2003). This wide range can be explained at least in part by the fact that the relationship between the AOD and PM depends on the particles optical properties, themselves controlled by their complex physical (size, shape, affinity with water vapour, etc.) and compositional characteristics. In some locations, the aerosols may also be frequently transported in elevated layers and thus be disconnected from the surface. In this case, their presence is detected by remote sensing techniques but not by the surface monitoring stations, which hinders the possibility of deriving PM from the AOD. In summary, the relationship between these two quantities must be evaluated for each climatic zone.

In this work, we propose to perform such an evaluation primarily for Cairo (Egypt) for which the available dataset is the longest and also for Delhi (India). The fact that the first site has a dry climate and the second one a tropical one will help test the influence of the climate on our results.

With its population of 24 million inhabitants, Cairo is located at the southern tip of the Nile Delta, has two desert areas on its west and east side (the Pyramids and the El-Mokattam plateaus, respectively), and is connected to the Nile River valley in the south. Because of the rapid growth of its population, associated urbanization, and industrialization in the second half of the last century, the city is suffering from high levels of air pollution and particularly PM (Abu-Allaban et al., 2007; Incecik & Im, 2012; Mostafa et al., 2019; Wheida et al., 2018). On a yearly basis, residential and transportation activities are the most significant sources of PM, emitting approximately 53 and 40% of particulate emissions, respectively (Incecik & Im, 2012). In autumn, the burning of agricultural waste in the Nile Delta is also an important source of particles transported towards Cairo by the prevailing northern winds. In springtime, the dust-laden winds blowing from the arid regions of Egypt (such as the Western and Eastern Deserts) are also significant contributors to the building up of the PM concentrations over the city (e.g. El-Metwally et al., 2008, 2010; Favez et al., 2008).

Similarly, the conurbation of Delhi counts 32 million inhabitants and is one of the most polluted megacities in the World (Rizwan et al., 2013). The levels of outdoor air pollution is particularly high in winter, which results in increased respiratory morbidity (Agarwal et al., 2006). More generally, India is largely exposed to the 'brown cloud', a layer of anthropogenic aerosols particularly enriched in black carbon and other light-absorbing particles produced by the combustion of fossil fuels and biomass burning (Alfaro et al., 2003; Lelieveld et al., 2001; Ramanathan et al., 2001). Moreover, these anthropogenic particles can occasionally mix with natural aerosols such as desert dust (Leon et al., 2001).

Section "Data and Methodology" gives more details on the available data and methods used in this study. The factors controlling the correlation between the surface PM and the AERONET AOD are analysed and discussed in section "Results and Discussion". Following this, a model is proposed and the evolution of the surface concentrations in Cairo between 2005 and 2022 is quantified.

Finally, the conclusions of our study are presented in section "Summary and Conclusion".

Data and Methodology

Theoretical Considerations

Sunphotometers operated from the Earth's surface as well as satellite-borne radiometers estimate the vertically integrated content of aerosols in the atmosphere from the modification of the field of radiance they induce. The result of this estimation is the aerosol optical depth (AOD) at a variable number of specific wavelengths (λ) in the spectral domain ranging from the UV to the near-infrared (NIR).

$$\mathrm{AOD}_{\lambda} = \int_{0}^{\mathrm{TOA}} C\sigma \, dz \tag{1}$$

In this expression, C (in kg m^{-3}) is the mass concentration of the aerosols in the atmospheric layer of elevation

z and depth dz, and σ (in $m^2\ kg^{-1}$) is their mass extinction efficiency at wavelength λ. The vertical integration is performed from the Earth's surface ($z = 0$) to the top of the atmosphere (TOA).

Under the assumption that the aerosols are transported close to the surface in the so-called mixed layer (ML, of depth H) and that the ML is homogenous, Eq. (1) simply reduces to:

$$\mathrm{AOD}_\lambda = \sigma HC \tag{2}$$

However simple, this equation shows that the AOD and C are not proportional in the strict sense. Firstly, H is typically of the order of several hundred metres, but it varies with the seasons and during the course of a given day because it depends on the surface solar irradiation, temperature, and wind speed. Secondly, σ depends on the size and composition of the aerosol particles. For instance, at 550 nm, σ varies between 3.3 and 3.7 $m^2\ g^{-1}$ for Saharan mineral dust (Linke et al., 2006) but is more variable for ambient elemental carbon (EC) with values ranging from 1.7 to 7.3 $m^2\ g^{-1}$ (Dillner et al., 2001). In the case of hydrophilic aerosols (e.g. sulphates or nitrates), the adsorption of water vapour at the surface of the particles increases their size and modifies their refractive index, which has a direct impact on σ.

In summary, the AOD/C ratio, whose value is necessary to retrieve the surface concentration from the measured AOD, is expected to vary with the nature of the aerosol and with the height and content in water vapour of the boundary layer. It will be seen below that Angström's exponent (AE) can be used as a proxy of the nature of the aerosol, that the content of the atmosphere in precipitable water (PW, in cm) is measured by the ground-based sunphotometers, and that reanalyses such as ERA5 provide estimates of H (in m).

Therefore, for any given location (Cairo and Delhi, in this study), a first-order development of Eq. (2) around the local mean values of AE, PW, and H yields:

$$\begin{aligned}\mathrm{AOD}/C = {} & s_{\mathrm{mean}} H_{\mathrm{mean}} (1 + C1(\mathrm{AE} - \mathrm{AE}_{\mathrm{mean}})) \\ & (1 + C2(\mathrm{PW} - \mathrm{PW}_{\mathrm{mean}}))(1 + C3(H - H_{\mathrm{mean}}))\end{aligned} \tag{3}$$

In this equation, σ_{mean} is the mass extinction efficiency of the average aerosol in humidity conditions corresponding to the mean of the period of study. The unknown C represents the sensitivities of the AOD/C ratio to variations of AE, PW, and H, respectively. $C1$ is unitless, $C2$ in cm^{-1}, and $C3$ in m^{-1}. Their values can be determined by application of a least square iterative routine used to provide the best fit of Eq. (3) to the measured values of AOD/C.

Measurements

Surface PM10 Mass Concentration

The hourly surface mass concentration data of Cairo and Gual Pahari were obtained from the WMO-GAW World Data Centre for Aerosols (WDCA) via the database infrastructure developed and operated by the Norwegian Institute for Air Research (https://ebas.nilu.no/).

These concentrations correspond to particles with aerodynamic diameters less than 10 µm (PM10). For Cairo, the measurements are those of the station located at the headquarters of the Egyptian Meteorological Authority (EMA) in El-Abbasiya (lat: 30.08 N; long: 31.29 E). The El-Abbasiya area is classified as an urban and residential location. At the station, the aerosol concentration is measured at 45 m above mean sea level with a beta-gauge sampler (Thermo Scientific SHARP Monitor, Model 5030, which combines light scattering photometry and beta-radiation attenuation). The current study analyses the data from June 2010 to May 2015, which are those posted in the EBAS archive.

In Gual Pahari (lat: 28.43 N; long: 77.15 E, 320 m amsl), the PM10 hourly surface concentration was measured with a Thermo Scientific beta-hybrid mass monitor from the end of 2008 to the beginning of 2010. The station, located about 25 km south of Delhi (in Gurgaon), was set up in the frame of the EUCAARI GAW-WDCA project (Hyvärinen et al., 2010). The measurements were also downloaded from the aforementioned NILU website. In this study, we use only the 2009 data because they are the least lacunar.

Finally, the daily means of the PM10 concentrations at the two sites were calculated from the hourly values.

AERONET Data

The Aerosol Robotics Network (AERONET) is a global, ground-based remote sensing network of automatic CIMEL sunphotometers maintained by the NASA. The instruments measure the direct sun and sky radiances at several wavelengths, and the spectral AOD is computed from these observations. The AERONET products are provided on the NASA website (https://aeronet.gsfc.nasa.gov/) at three quality levels. In this study, we use only the cloud-screened (Level 1.5) and cloud-screened and quality-assured (Level 2) products.

At the El-Abbasiya station, a first instrument was operated from April 2005 to March 2006 (Cairo_EMA) and then a second one (Cairo_EMA_2) from April 2010 to today but with a notable interruption from July 2019 to January 2021. The CIMEL instruments are automatic

multispectral sun-tracking photometers. For instance, the CE-318 model of Cairo_EMA_2 performs sun measurements in eight spectral bands: 340, 380, 440, 500, 670, 870, 940, and 1020 nm. The 940 nm wavelength is dedicated to the evaluation of the columnar content of the atmosphere in precipitable water vapour (PW) and the others to that of the AOD. At Gual Pahari, Aeronet measurements were taken in parallel with the surface PM concentrations from the end of 2008 to the beginning of 2010. In this study, we use the data of 2009 that are the most complete.

The spectral dependence of this AOD can be quantified by the means of the Angström exponent (AE), which provides useful information on the type of aerosol present in the atmospheric column (El-Metwally et al., 2008; Masmoudi et al., 2015). Indeed, low AEs are associated with coarse (supermicron) dust-like particles, whereas large AEs correspond to finer (submicron) aerosols of anthropic origin (El-Metwally et al., 2020).

AE is obtained by the Volz method as in Abou El-Magd et al. (2020):

$$\begin{aligned} \mathrm{AE} &= -d\ln(\tau)\backslash d\ln(\lambda) \\ &= -\ln(\tau_1\backslash\tau_2)\backslash\ln(\lambda_1\backslash\lambda_2) \end{aligned} \tag{4}$$

where τ_1 and τ_2 are the AODs at two different wavelengths (500 and 675 nm, in the following).

For consistency with many studies that retain 550 nm as their reference wavelength, we used the AE to derive the AERONET AOD at 550 nm from that measured at 500 nm.

Finally, the number of days with synchronous concentration and AOD measurements is 1487 for the Egyptian site and 246 for the Indian one. The missing data are due to interruption of the measurements for instrumental maintenance or because of the days during which the sunphotometer measurements were either not taken (cloudy days) or did not pass the quality-check requirements.

ERA5 Reanalysis Data

The boundary layer height is very rarely measured directly at meteorological stations. *H* could be estimated from the surface roughness and such meteorological quantities as the surface temperature, solar irradiation, and wind speed, but it can also be obtained more simply as one of the numerous products of the ERA5 (Hersbach et al., 2020) reanalysis of the European Centre for Medium-Range Weather Forecast (ECMWF). In a reanalysis, an unchanging data assimilation system is used to provide a consistent reprocessing of all available observations. Because of their continuous spatial and temporal high-quality resolutions, such reanalyses are widely used in climate change studies (Delgado-Bonal et al., 2020; Engdaw et al., 2021; Molina et al., 2021). The ERA5 hourly *H* for Cairo and Gual Pahari was downloaded from the Copernicus Climate Change Service Climate Data Store (CDS): (https://cds.climate.copernicus.eu/cdsapp#!/home) and used to calculate the daily averages.

Results and Discussion

Temporal Variabilities of the AOD and Surface Concentration

The daily averages of the AOD (Fig. 1a) measured at the Cairo_EMA_2 station in the period 2010–2015 vary from about 0.10 to almost 2.0, with a mean of 0.36. The lowest AODs of the year were recorded in winter—probably because of the washing out of the aerosols by the rains that can occur in this season—but these minima coexist with much larger values. Summer is less variable and characterized by relatively low AODs. Conversely, sharp AOD peaks are common in autumn and particularly in spring. In good agreement with past studies (e.g. El-Metwally et al., 2008), the seasonal variations of the Angström exponent (Fig. 1b) and its correlation with the AOD (Fig. 2) provide useful hindsight on the origin of these peaks: the advection of desert dust in spring causes at the same time a significant reduction of the AE and an increase of the AOD. In absence of massive inputs of coarse dust, the composition of the aerosol is dominated by smaller particles of anthropogenic origin whose accumulation leads to the formation of AODs peaks associated with AEs around 1.4 (Fig. 2). Finally, the largest AEs (> 1.5) coincide with the moderate AODs of the summer period. They could indicate the formation of very small particles by photochemical reactions.

Close to the surface, the daily PM10 concentrations generally vary between 57 and 197 $\mu g\ m^{-3}$ (10th and 90th percentiles, respectively) but can occasionally largely exceed 500 $\mu g\ m^{-3}$ (Fig. 1c). With minima in summer and peaks in autumn, winter, and particularly spring, there are strong commonalities in the seasonality of *C* and the AOD.

At Gual Pahari, the AOD varied between 0.1 and about 2.0 (Fig. 1d), as in Cairo, but its yearly mean was larger (0.58, as compared to 0.36). In spite of a large day-to-day variability, there is no obvious seasonal dependence of the AOD during the period of study. In particular, the rains of the summer monsoon season do not have any apparent effect on the AOD, whereas they clearly tend to abate the surface PM10 concentrations (Fig. 1f). Finally, the lowest values of the AE are measured in June (Fig. 1d), just before the onset of the monsoon. These low AEs are associated with desert dust advected from the Thar Desert and adjoining regions (Pandithurai et al., 2008).

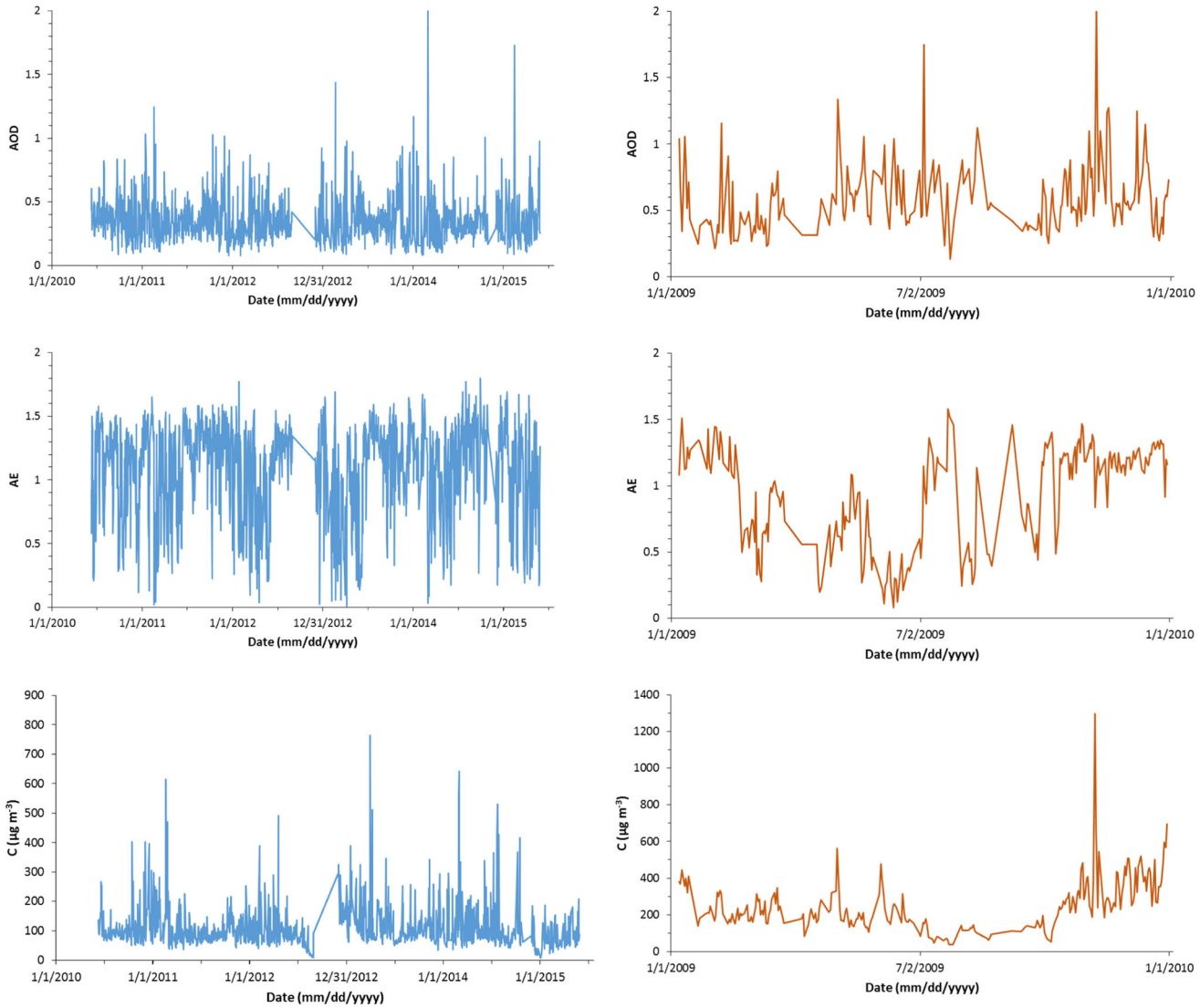

Fig. 1 From top to bottom, temporal evolutions of the AOD, Angström exponent (AE), and PM10 surface concentration (*C*) at the Cairo (left panels) and Gual Pahari (right panels) stations

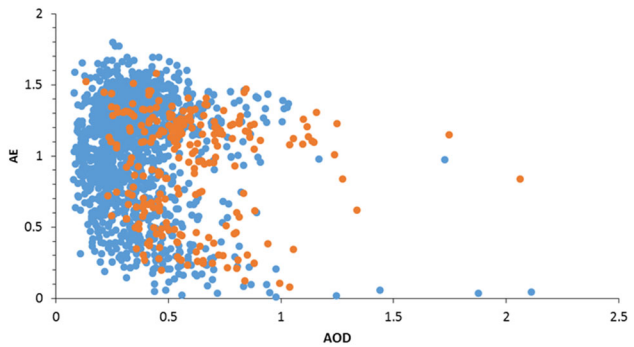

Fig. 2 Correlation between the AE and the AOD at the Cairo (blue points) and Gual Pahari (orange points) experimental stations

Variability of the AOD/*C* Ratio

The examination of the AOD/*C* temporal plots (Fig. 3a, b) shows that, at the two sites, this ratio tends to be the lowest in winter and to achieve its largest values in summer. The frequency distributions (Fig. 3c) also indicate that AOD/*C* is generally larger and more variable in Cairo (4.0 ± 2.7 10^{-3} m^3 μg^{-1}) than in Gual Pahari (3.0 ± 2.2 10^{-3} m^3 μg^{-1}). In the 5 years of the Cairo measurements, August 2012 and December 2014 are characterized by abnormally large AOD/*C* in the sense that they exceed the mean + 1 standard deviation value. These outliers can most probably be explained by aerosol transported in the free atmosphere. A similar situation is possibly observed in at the Indian site in summer, when the AOD/*C* ratio becomes particularly large. In these cases, the assumption

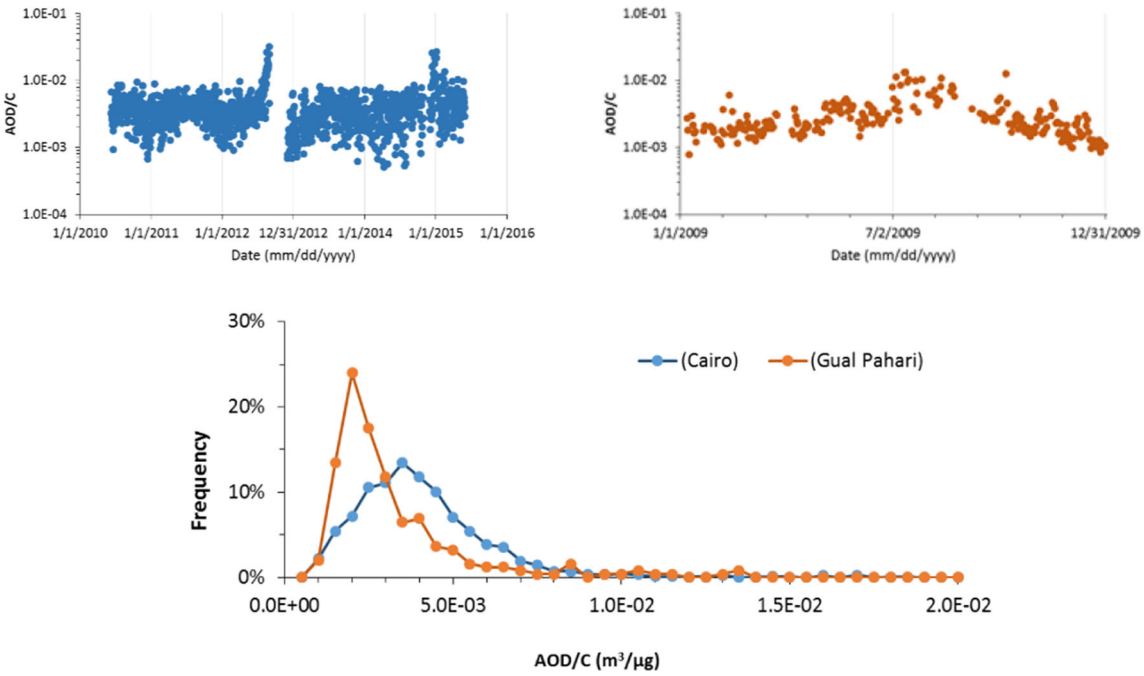

Fig. 3 Temporal variations of the AOD/*C* ratio (in $m^3\ \mu g^{-1}$) at the Cairo (upper left) and Gual Pahari (upper right) stations. The frequency distributions of the AOD/*C* values at the 2 sites are also compared (bottom panel)

underlying Eqs. (2) and (3), namely that the aerosol is confined to the mixed layer, does not stand. Therefore, these outliers will not be considered when adjusting Eq. (3) to the observations. The reassuring point for the development of our method is that this transport of the aerosol particles in elevated layers is rather rare. In other words, the AOD is usually controlled by the aerosols of the mixed layer, which is consistent with the fact that in megacities such as Cairo and Delhi the most active sources of particles are close to the surface.

Modelling of AOD/*C* and *C*

Table 1 reports the averages and relative standard deviations of AE, PW, and *H* for Cairo and Gual Pahari. The values of $(\sigma H)_{\text{mean}}$, *C*1, *C*2, and *C*3 obtained by adjustment of Eq. (3) to the measurements are also indicated. Finally, the range of variability (in %) of AOD/*C* that can be attributed to the variations of the AE, PW, and *H* considered individually are given by the means of their 10th and 90th percentiles.

The average PW at Gual Pahari (1.79 cm) compares to that of Cairo (1.90 cm), but it is more variable (50 and 33%, respectively). This is due to the large atmospheric contents in water vapour measured during the monsoon period at the Indian site. Regarding AE, it is only slightly larger in Cairo ($1.10 \pm 34\%$) than in Gual Pahari ($0.91 \pm 41\%$). These relatively large values are indicative of an aerosol dominated by fine particles of anthropogenic aerosols, which was to be expected in megacities.

The most striking result is the predominant influence of PW. In Cairo, its variations explain 16% of the variability of the AOD/*C* ratio. This proportion is even larger (up to 46%) in Gual Pahari because on the one hand PW is more variable than in Cairo, but on the other hand also because the sensitivity of the aerosol to PW (quantified by *C*2) is larger at the Indian site ($0.35\ cm^{-1}$) than at the Egyptian one ($0.23\ cm^{-1}$). This denotes a more pronounced hydrophilic character of the aerosol in the Delhi conurbation.

By contrast, the impact of the variations of the boundary layer height, which does not exceed 6% in Gual Pahari and 2% in Cairo, appears as rather limited. Finally, the influence of the AE is negligible at Gual Pahari (about 3% variability) but more significant in Cairo (almost 10%). One can hypothesize that for a less hydrophilic aerosol such as the Egyptian one, the impact of the variability of the particles' size on AOD/*C* is easier to detect because it is not masked by the overwhelming competing effect of hygroscopic growth.

Finally, the average mass extinction efficiencies of the Cairo aerosol ($5.59\ m^2\ g^{-1}$) are larger than that of Gual Pahari ($4.14\ m^2\ g^{-1}$). However, it must be noted that these values, which were obtained by dividing the product $(\sigma H)_{\text{mean}}$ by the ERA5 estimate of H_{mean}, depend on the accuracy of this estimate of the boundary layer height by the reanalysis. Moreover, these averages are only indicative in the sense that they do not reflect the important day-

Table 1 Comparison of the averages and relative standard deviations of the aerosol Angström exponent (AE), precipitable water vapour (PW), and boundary layer height (H) at the two experimental sites

	Cairo				Gual Pahari			
		AE	PW (cm)	H (m)		AE	PW (cm)	H (m)
Average		1.10	1.90	674		0.91	1.79	580
rSD (%)		34	27	33		41	52	50
	σH_{mean} (m^3 μg^{-1})	$C1$	$C2$ (cm^{-1})	$C3$ (m^{-1})	σH_{mean} (m^3 μg^{-1})	$C1$	$C2$ (cm^{-1})	$C3$ (m^{-1})
	$3.77\ 10^{-3}$	0.18	0.23	$6.47\ 10^{-5}$	$2.40\ 10^{-3}$	− 0.06	0.35	$-1.29\ 10^{-4}$
Centile (%)		$C1\Delta AE$	$C2\Delta PW$	$C3\Delta H$		$C1\Delta AE$	$C2\Delta PW$	$C3\Delta H$
0.1		− 9.9	− 16.8	− 1.8		− 2.4	− 34.9	− 6.1
0.5		1.8	0.9	0.2		− 0.6	− 6.5	0.9
0.9		6.4	16.0	1.6		3.3	46.4	4.2

The coefficients σH_{mean}, $C1$, $C2$, and $C3$ were obtained by adjustment of Eq. (3) to the measurements. The 10th, 50th, and 90th percentiles of the variability of the AOD/C ratio attributable to variations of the AE, PW, and H are also reported

to-day variability of the aerosol composition denoted by the variations of AE.

Once the coefficients of Eq. (3) have been determined, the computation of the daily C from the AOD, PW, AE, and H is straightforward. Hereinafter, this calculated value will be referred to as $C_{model,1\ day}$. The comparison of $C_{model,1\ day}$ with the observations allows assessing the quality of the model by the means of metrics such as the root-mean-square error (RMSE), relative mean absolute error (rMAE), and correlation coefficient (R). The same method can be applied after averaging of the daily values in sliding windows of width 7 or 30 days.

The results of these comparisons are reported in Table 2 along with the average PM10 concentrations and numbers of daily observations for the 2 experimental sites. They show that the performance of the model improves with the duration of the width of the averaging period. For instance, rMAE is 26% for Cairo and 21% for Gual Pahari at the daily temporal resolution, but it drops to 15 and 12% (respectively) at the 7-day resolution. In the meantime, R increases significantly to reach values above 0.8, particularly at Gual Pahari (R = 0.87). At the monthly resolution, the results are even better with rMAE and R of 11% and 0.86 at Cairo and 5% and 0.96 at Gual Pahari. In summary, the model based on Eq. (3) is quite able to simulate the variability of the surface PM concentration and particularly at the weekly and monthly resolutions. To illustrate this point further, Fig. 4 compares the temporal evolutions of the modelled and observed surface concentrations at the 2 experimental sites of this study.

Table 2 Number of daily observations (N_{obs}) and average concentration ($C_{ave.}$, in $\mu g\ m^{-3}$) at the 2 experimental sites

	Cairo			Gual Pahari		
N_{obs}	1287			220		
$C_{ave.}$	106			259		
Averaging (days)	1	7	30	1	7	30
RMSE	42.0	21.4	16.7	83.2	47.4	23.2
rMAE	26	15	11	21	12	5
R	0.74	0.81	0.86	0.79	0.87	0.96

The concentrations calculated with Eq. (3) are compared to the observations after averaging over sliding windows of width 1, 7, and 30 days. The goodness of fit is quantified by the means of the root-mean-square error (RMSE, in $\mu g\ m^{-3}$), relative mean absolute error (rMAE, in %), and correlation coefficient (R)

PM Trend in Cairo

However, discontinuous, Aeronet measurements have been taken in Cairo since 2005. Therefore, it is possible to reconstruct the evolution of the PM10 surface concentration over a much longer period than that considered in Fig. 4. The results (Fig. 5) confirm the important seasonal and interannual variability of C. However, no significant trend (R^2 = 0.003) is observed in the last 18 years of available data. Noteworthy, it can be regretted that the sunphotometer measurements were interrupted in 2020 for re-calibration of the instrument. This would have allowed documenting the impact of the COVID lockdown on the levels of particulate pollution to which the population is exposed.

Summary and Conclusion

In this study we have analysed the correlation between the daily averages of the PM10 surface concentrations (C) monitored in two megacities with contrasted climates

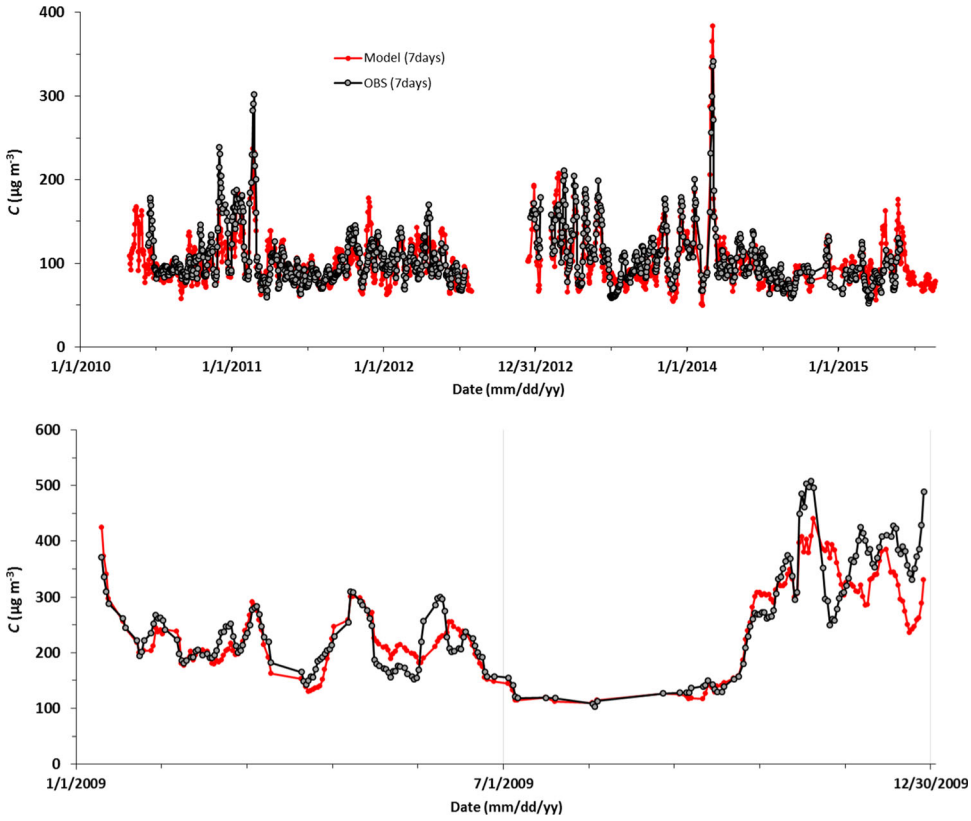

Fig. 4 Comparison of the modelled surface concentration (red curve) with the observations (black curve) of the Cairo and Gual Pahari experimental stations (upper and lower panels, respectively). The width of the averaging window is 7 days

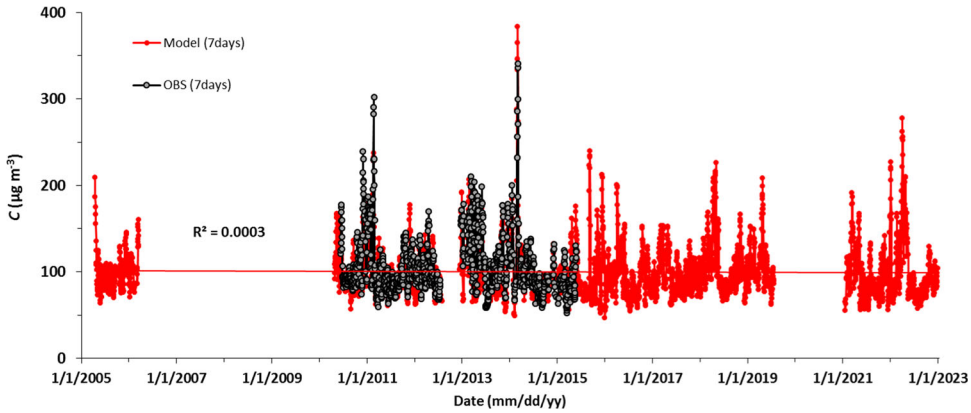

Fig. 5 Extension of Fig. 4 to the whole period of Aeronet measurements available in Cairo. The horizontal red line is the best fit to the modelled concentrations and shows that there was no significant evolution of these concentrations in the last 18 years (R^2 = 0.0003)

(Cairo and Gual Pahari, in the Delhi conurbation) and the AOD measured by collocated sunphotometers of the Aerosol Robotics Network.

At the two sites, the variations of the AOD/*C* ratio are driven in the first place by the atmospheric content in precipitable water vapour (PW), which emphasizes the hygroscopic nature of the aerosol at the two locations. However, that this effect is more pronounced at the Indian site than at the Egyptian one indicates differences in aerosols composition and affinity with water vapour.

Besides humidity, variations of the Angström exponent (AE) used as a proxy of the size of the aerosol particles have a significant impact on AOD/*C* in Cairo but not in Gual Pahari. At the latter site, the influence of the variations of the particles size is most probably masked by the overwhelming effect of humidity.

Finally, the variability of the planetary boundary layer height (*H*), is found to play only a secondary role at the two locations.

At the daily temporal resolution, a simple model (Eq. (3)) derived from these observations allows retrieving the measured *C* with an accuracy of 26 and 21% (relative mean absolute error) Cairo and Gual Pahari. This agreement is considerably improved at the weekly (15 and 12%, respectively) and monthly (11 and 5%) resolutions. The

correlation coefficients are then better than 0.81 at the 2 sites.

This very good agreement of this empirical model with observations shows that Aeronet measurements are a perfect tool for estimating the surface concentrations in megacities. It also validates indirectly the main assumption of the model, namely that the aerosol particles are in most cases confined to the PBL. Because the capping inversion at the top of the PBL usually acts as a barrier preventing the passage of the particles towards the free atmosphere, this confinement was expected in megacities where the majority of the aerosol sources (cars, industries, waste burning, etc.) are located very close to the Earth's surface. However, in some regions, aerosols transported at high altitudes could constitute an exception. For instance, previous studies showed that desert dust can be transported over the Mediterranean under the form of layered plumes in the free atmosphere (e.g. Denjean et al., 2016; Di Sarra et al., 2001; Gkikas et al., 2016), especially in summer when intense convection facilitates the initial vertical uplift of the dust particles above the source regions. The fact that in Egypt and India the production of mineral dust does not occur in summer but mostly in springtime (when solar radiation is less intense) could explain that it does not reach the free atmosphere.

Finally, the methodology applied in this work could easily be applied for any other AERONET station where at least a few years of parallel measurements of the surface concentration are available. These direct measurements are necessary for checking the validity of the model's assumptions and for its calibration.

Acknowledgements The authors are grateful to STDF Egypt for their support to project No 43088, and the PIs (Africa Barreto and Ashraf S. Zakey for Cairo_EMA_2; Anti Arola for Gual Pahari) of the AERONET sites and to the staff who maintain it. The authors are also grateful to the Egyptian Meteorological Authority and Finnish Meteorological Institute for providing the PM10 data through the WMO/GAW World Data Center of Aerosols hosted by Norwegian Institute for Air Research-NILU (http://ebas-data.nilu.no/). The authors are thankful to the ECMWF for providing ERA-5 data: (Fifth generation of ECMWF atmospheric reanalyses of the global climate) through Copernicus Climate Change Service Climate Data Store (CDS).

Funding Open access funding provided by The Science, Technology & Innovation Funding Authority (STDF) in cooperation with The Egyptian Knowledge Bank (EKB).

Declaration

Conflict of interest The authors declared that they have no conflict of interest.

References

Abou El-Magd, I., Zanaty, N., Ali, E. M., Irie, H., & Abdelkader, A. I. (2020). Investigation of aerosol climatology, optical characteristics and variability over Egypt based on satellite observations and in-situ measurements. *Atmosphere, 11*, 714–719. https://doi.org/10.3390/atmos11070714

Abu-Allaban, M., Lowenthal, D., Gertler, A., & Labib, M. (2007). Sources of PM10 and PM2.5 in Cairo's Ambient Air. *Environmental Monitoring and Assessment, 133*, 417–425.

Agarwal, R., Jayaraman, G., Anand, S., & Marimuthu, P. (2006). Assessing respiratory morbidity through pollution status and meteorological conditions for Delhi. *Environmental Monitoring and Assessment, 114*, 489–504. https://doi.org/10.1007/s10661-006-4935-3

Alfaro, S. C., Gaudichet, A., Rajot, J. L., Gomes, L., Maillé, M., & Cachier, H. (2003). Variability of aerosol size resolved composition at an Indian coastal site during the INDOEX intensive field phase. *Journal of Geophysical Research*. https://doi.org/10.1029/2002JD002645,2003

Alfaro, S. C., & Wahab, M. A. (2006). Extreme variability of aerosol optical properties: The Cairo aerosol characterization experiment case study. *NATO Security through Science Series*. https://doi.org/10.1007/978-1-4020-5090-9_1

Barladeanu, R., Stefan, S., & Radulescu, R. (2012). Correlation between the particulate matter (PM10) mass concentrations and aerosol optical depth in Bucharest, Romania. *Romanian Reports in Physics, 64*, 1085–1096.

Brauer, M., Amann, M., Burnett, R. T., Cohen, A., Dentener, F., Ezzati, M., Henderson, S. B., Krzyzanowski, M., Martin, R. V., Van Dingenen, R., van Donkelaar, A., & Thurston, G. D. (2012). Exposure assessment for estimation of the global burden of disease attributable to outdoor air pollution. *Environmental Science and Technology, 46*, 652–660. https://doi.org/10.1021/es2025752

Brook, R., Rajagopalan, S., Pope, C., Brook, J., Bhatnagar, A., Diez Roux, A., Holguin, F., Hong, Y., Luepker, R., Mittleman, M., Peters, A., Siscovick, D., Smith, S., Whitsel, L., & Kaufman, J. (2010). Particulate matter air pollution and cardiovascular disease an update to the scientific statement from the American Heart Association. *Circulation, 121*, 2331–2378. https://doi.org/10.1161/CIR.0b013e3181dbece1

Chu, D. A., Kaufman, Y. J., Zibordi, G., Chern, J. D., Mao, J., Li, C., & Holben, B. N. (2003). Global monitoring of air pollution over land from EOS-Terra MODIS. *Journal of Geophysical Research, 108*(D21), 4661. https://doi.org/10.1029/2002JD003179

Delgado-Bonal, A., Marshak, A., Yang, Y., & Holdaway, D. (2020). Analyzing changes in the complexity of climate in the last four decades using MERRA-2 radiation data. *Scientific Reports, 10*, 922. https://doi.org/10.1038/s41598-020-57917-8

Denjean, C., Cassola, F., Mazzino, A., Triquet, S., Chevaillier, S., Grand, N., Bourrianne, T., Momboisse, G., Sellegri, K., Schwarzenbock, A., Freney, E., Mallet, M., & Formenti, P.

(2016). Size distribution and optical properties of mineral dust aerosols transported in the western Mediterranean. *Atmospheric Chemistry and Physics, 16*(2), 1081–1104. https://doi.org/10.5194/acp-16-1081-2016

Di Sarra, A., Di Iorio, T., Cacciani, M., Fiocco, G., & Fua, D. (2001). Saharan dust profiles measured by lidar at Lampedusa. *Journal of Geophysical Research: Atmospheres, 106*(D10), 10335–10347.

Dillner, A. M., Stein, C., Larson, S. M., & Hitzenberger, R. (2001). Measuring the mass extinction efficiency of elemental carbon in rural aerosol. *Aerosol Science and Technology, 35*(6), 1009–1021. https://doi.org/10.1080/027868201753306778

El-Metwally, M., Alfaro, S. C., Abdel Wahab, M., & Chatenet, B. (2008). Aerosol characteristics over urban Cairo: Seasonal variations as retrieved from Sun photometer measurements. *Journal of Geophysical Research, 113*, D14219. https://doi.org/10.1029/2008JD009834

El-Metwally, M., Alfaro, S. C., Wahab, M. A., Zakey, A. S., & Chatenet, B. (2010). Seasonal and inter-annual variability of the aerosol content in Cairo (Egypt) as deduced from the comparison of MODIS aerosol retrievals with direct AERONET measurements. *Atmospheric Research, 97*(1–2), 14–22.

El-Metwally, M., Korany, M., Boraiy, M., Ebada, E., Abdel Wahab, M. M., Hungershoefer, K., & Alfaro, S. C. (2020). Evidence of anthropization of aerosols in the Saharan and peri-Saharan regions: implications for the atmospheric transfer of solar radiation. *Journal of Atmospheric and Solar-Terrestrial Physics*. https://doi.org/10.1016/j.jastp.2020.105199

Engdaw, M. M., Ballinger, A. P., Hegerl, G. C., & Steiner, A. K. (2021). Changes in temperature and heat waves over Africa using observational and reanalysis data sets. *International Journal of Climatology*. https://doi.org/10.1002/joc.7295

Engel-Cox, J. A., Hoff, R. M., & Haymet, A. D. J. (2004). Recommendations on the use of satellite remote-sensing data for urban air quality. *Journal of the Air & Waste Management Association, 54*(11), 1360–1371. https://doi.org/10.1080/10473289.2004.10471005

Favez, O., Cachier, H., Sciare, J., Alfaro, S., El-Araby, T., Harhash, M., & Abdelwahab, M. (2008). Seasonality of major aerosol species and their transformations in Cairo megacity. *Atmospheric Environment, 42*, 1503–1516.

Gkikas, A., Basart, S., Hatzianastassiou, N., Marinou, E., Amiridis, V., Kazadzis, S., & Baldasano, J. M. (2016). Mediterranean intense desert dust outbreaks and their vertical structure based on remote sensing data. *Atmospheric Chemistry and Physics, 16*, 8609–8642.

Grguric, S., Krizan, J., Gasparae, G., Antonic, O., Spiric, Z., Mamouri, E. R., Christodoulou, A., Nisantzi, A., Agapiou, A., Themistocleous, K., Fedra, K., Panaylotou, C., & Hadjilmitsis, D. (2014). Relationship between MODIS based Aerosol optical depth and PM10 over Croatia. *Central European Journal of Geosciences, 6*(1), 2–16. https://doi.org/10.2478/s13533-012-0135-6

Guo, J., Xia, F., Zhang, Y., Liu, H., Li, J., Lou, M., He, J., Yan, Y., Wang, F., Min, M., & Zhai, P. (2017). Impact of diurnal variability and meteorological factors on the PM2.5-AOD relationship: Implications for PM2.5 remote sensing. *Environmental Pollution, 221*, 94–104. https://doi.org/10.1016/j.envpol.2016.11.043

Gupta, P., & Christopher, S. A. (2008). Seven year particulate matter air quality assessment from surface and satellite measurements. *Atmospheric Chemistry and Physics, 8*, 3311–3324. https://doi.org/10.5194/acp-8-3311-2008

Handschuh, J., Erbertseder, T., Schaap, M., & Baier, F. (2022). Estimating PM2.5 surface concentrations from AOD: A combination of SLSTR and MODIS. *Remote Sensing Applications: Society and Environment, 26*, 100716. https://doi.org/10.1016/j.rsase.2022.100716

Hersbach, H., Bell, B., Berrisford, P., Hirahara, S., Horányi, A., Muñoz-Sabater, J., Nicolas, J., Peubey, C., Radu, R., Schepers, D., Simmons, A., Soci, C., Abdalla, S., Abellan, X., Balsamo, G., Bechtold, P., Biavati, G., Bidlot, J., Bonavita, M., … Thépaut, J.-N. (2020). The ERA5 global reanalysis. *Quarterly Journal of the Royal Meteorological Society, 146*, 1999–2049. https://doi.org/10.1002/qj.3803

Hyvärinen, A.-P., Lihavainen, H., Komppula, M., Panwar, T. S., Sharma, V. P., Hooda, R. K., & Viisanen, Y. (2010). Aerosol measurements at the Gual Pahari EUCAARI station: Preliminary results from in-situ measurements. *Atmospheric Chemistry and Physics, 10*, 7241–7252. https://doi.org/10.5194/acp-10-7241-2010

Incecik, S., & Im, U. (2012). Air pollution in mega cities: a case study of Istanbul. *Air pollution–monitoring, modeling and health* (pp. 77–116). InTech.

Kim, K. H., Kabir, E., & Kabir, S. (2015). A review on the human health impact of airborne particulate matter. *Environment International, 74*, 136–143.

Kong, L., Xin, J., Zhang, W., & Wang, Y. (2016). The empirical correlations between PM2.5, PM10 and AOD in the Beijing metropolitan region and the PM2.5, PM10 distributions retrieved by MODIS. *Environmental Pollution, 21*, 350–360. https://doi.org/10.1016/j.envpol.2016.05.085

Lelieveld, J., et al. (2001). The Indian ocean experiment: Widespread air pollution from South and Southeast Asia. *Science, 291*, 1031–1036.

Leon, J.-F., Chazette, P., Dulac, F., Pelon, J., Flamant, C., Bonazzola, M., Foret, G., Alfaro, S. C., Cachier, H., Cautenet, S., Hamonou, E., Gaudichet, A., Gomes, L., Rajot, J.-L., Lavenu, F., Inamdar, S. R., Sarode, P. R., & Kadadevarmath, J. S. (2001). Large scale advection of continental aerosols during INDOEX. *Journal of Geophysical Research: Atmospheres, 106*(D22), 28427–28439.

Linke, C., Möhler, O., Veres, A., Mohácsi, Á., Bozóki, Z., Szabó, G., & Schnaiter, M. (2006). Optical properties and mineralogical composition of different Saharan mineral dust samples: A laboratory study. *Atmospheric Chemistry and Physics, 6*, 3315–3323. https://doi.org/10.5194/acp-6-3315-2006

Lv, M., Liu, D., Li, Z., Mao, J., Sun, Y., Wang, Z., Wang, Y., & Xie, C. (2017). Hygroscopic growth of atmospheric aerosol particles based on lidar, radiosonde, and in situ measurements: Case studies from the Xinzhou field campaign. *Journal of Quantitative Spectroscopy and Radiative Transfer, 188*, 60–70. https://doi.org/10.1016/j.jqsrt.2015.12.029

Ma, X., Wang, J., Yu, F., Jia, H., & Hu, Y. (2016). Can MODIS AOD be employed to derive PM2.5 in Beijing–Tianjin–Hebei over China? *Atmospheric Research, 181*, 250–256. https://doi.org/10.1016/j.atmosres.2016.06.018

Masmoudi, M., Alfaro, S. C., & El-Metwally, M. (2015). A comparison of the physical properties of desert dust retrieved from the sunphotometer observation of major events in the Sahara, Sahel, and Arabian Peninsula. *Atmospheric Research, 158–159*, 24–35. https://doi.org/10.1016/j.atmosres.2015.02.005

Molina, M. O., Gutiérrez, C., & Enrique Sánchez, E. (2021). Comparison of ERA5 surface wind speed climatologies over Europe with observations from the HadISD dataset. *International Journal of Climatology*. https://doi.org/10.1002/joc.7103

Mostafa, A. N., Zakey, A. S., Alfaro, S. C., Wheida, A. A., Monem, S. A., & Abdul Wahab, M. M. (2019). Validation of RegCM-CHEM4 model by comparison with surface measurements in the Greater Cairo (Egypt) megacity. *Environmental Science and Pollution Research, 26*(23), 23524–23541.

Pandithurai, G., Dipu, S., Dani, K. K., Tiwari, S., Bisht, D. S., Devara, P. C. S., & Pinker, R. T. (2008). Aerosol radiative forcing during

dust events over New Delhi, India. *Journal of Geophysical Research: Atmospheres*, *113*(D13).

Prescott, G. J., Cohen, G. R., Elton, R. A., Fowkes, F. G., & Agius, R. M. (1998). Urban air pollution and cardiopulmonary ill health: A 14.5 year time series study. *Occupational and Environmental Medicine, 55*, 697–704.

Ramanathan, V., et al. (2001). Indian Ocean experiment: An integrated analysis of the climate forcing and effects of the great Indo-Asian hase. *Journal of Geophysical Research, 106*(D22), 28371–28398.

Ramanathan, V., Crutzen, P., Kiehl, J., & Rosenfeld, D. (2002). Aerosols, climate, and the hydrological cycle. *Science, 294*, 2119–2124. https://doi.org/10.1126/science.1064034

Rizwan, S., Nongkynrih, B., & Gupta, S. K. (2013). Air pollution in Delhi: Its magnitude and effects on health. *Indian J Community Medicine, 38*(1), 4–8. https://doi.org/10.4103/0970-0218.106617.PMID:23559696;PMCID:PMC3612296

Sokolik, I. N., & Toon, O. B. (1996). Direct radiative forcing by anthropogenic airborne mineral aerosols. *Nature, 381*, 681–683.

Wang, J., & Christopher, S. A. (2003). Intercomparison between satellite-derived aerosol optical thickness and PM2.5 mass: Implications for air quality studies. *Geophysical Research Letters, 30*(21), 2095. https://doi.org/10.1029/2003GL018174

Wheida, A., Nasser, A., El-Nazer, M., Borbon, A., Abo El Ata, G. A., Abdel Wahab, M., & Alfaro, S. C. (2018). Tackling the mortality from long-term exposure to outdoor air pollution in megacities: Lessons from the Greater Cairo case study. *Environmental Research, 2018*(160), 223–231.

Yahi, H., Marticorena, B., Thiria, S., Chatenet, B., Schmechtig, C., Rajot, J. L., & Crepon, M. (2013). Statistical relationship between surface PM10 concentration and aerosol optical depth over the Sahel as a function of weather type, using neural network methodology. *Journal of Geophysical Research: Atmospheres, 118*, 13265–13281. https://doi.org/10.1002/2013JD019465

You, W., Zang, Z., Zhang, L., Zhang, M., Pan, X., & Li, Y. (2016). A nonlinear model for estimating ground-level PM10 concentration in Xi'an using MODIS aerosol optical depth retrieval. *Atmospheric Research, 168*, 169–179.

Zhang, Y., Li, Z., Bai, K., Wei, Y., Xie, Y., Zhang, Y., Ou, Y., Cohen, J., Zhang, Y., Peng, Z., Zhang, X., Chen, C., Hong, J., Xu, H., Guang, J., Lv, Y., Li, K., & Li, D. (2021). Satellite remote sensing of atmospheric particulate matter mass concentration: advances, challenges, and perspectives. *Fundamental Research, 1*(3), 240–258.